

# Impact of Autonomous Vehicles on the Car-Following Behaviour of Human Drivers

Ruixuan Zhang<sup>1,2</sup>, Sara Masoud<sup>3</sup>, and Neda Masoud<sup>4</sup>

<sup>1</sup>Graduate Research Assistant, Civil and Environmental Engineering, University of Michigan Ann Arbor, Address: 2350 Hayward St, Ann Arbor, MI 48109, Email: ruixuanz@umich.edu

<sup>2</sup>Intern, Advanced Engineering, Isuzu Technical Center of America, Address: 46401 Commerce Center Dr, Plymouth, MI 48170, Email: ruixuan.zhang@isza.com

<sup>3</sup>Assistant Professor, Industrial and Systems Engineering, Wayne State University, Address: 4815  
4th St, Detroit, MI 48201, Email: saramasoud@wayne.edu

<sup>4</sup>Assistant Professor, Civil and Environmental Engineering, University of Michigan Ann Arbor,  
Address: 2350 Hayward St, Ann Arbor, MI 48109, Email: [nmasoud@umich.edu](mailto:nmasoud@umich.edu)

## ABSTRACT

The past few years have witness to an increase in autonomous vehicle (AV) development and testing. However, even with a fully developed and comprehensively tested AV technology, AVs are anticipated to share the roadway network with human drivers for the unforeseeable future. In such a mixed environment, we use naturalistic driving data from the Next Generation Simulation (NGSIM) and Lyft Level 5 (Lyft L5) prediction datasets to investigate whether the existence of AVs influences the car following behavior of human drivers. We use time headway time series as a proxy to capture the car following behaviour of human drivers. We then develop a nested fixed model to find possible changes in behaviour when human drivers are following different types of vehicles (i.e., human-driven vehicles or AVs). The factors included in this model are the platoon structure (a legacy vehicle following a legacy vehicle, and a legacy vehicle following an autonomous vehicle), road type (freeway and urban), time period (morning and afternoon), lane (right, middle,

24 and left), and the source of the data (NGSIM and Lyft L5). Results indicate a statistically significant  
25 difference between the car following behaviour of drivers when they follow a human-driven vehicle  
26 compared to an AV. This change in the car following behaviour of drivers is manifested in the form  
27 of a reduction in the mean and variance of time headways when human drivers follow an AV. These  
28 findings can bridge the gap between anticipated and real-world impacts of AVs on traffic streams  
29 and roadway stability and capacity, providing meaningful insights on the influence of AVs on the  
30 driving behavior of humans in a naturalistic driving environment.

31 **Author keywords:** Autonomous vehicle-human driver interactions, Car-following behaviour

## 32 INTRODUCTION

33 The past few years have been a witness to an increase in autonomous vehicle (AV) development  
34 and testing, with many mobility-oriented companies as well as original equipment manufacturers  
35 (OEMS) attempting to either open AV divisions or partner with/acquire start-ups that focus on  
36 software or hardware development for AVs. This move toward a future autonomous transportation  
37 system is fueled by many anticipated benefits of AVs, such as increased safety and smoother traffic  
38 flow (Zhang et al. 2022a; Wyk et al. 2019; Zhang et al. 2022b; Zhang et al. 2021), which in turn  
39 leads to higher levels of fuel economy, less congestion, a wider range of mobility options, and  
40 curbing the environmental footprint of the transportation sector (Stern et al. 2018; Liu et al. 2020b;  
41 Liu et al. 2020a; Zhang et al. 2020; Ersal et al. 2020; Masoud and Jayakrishnan 2017; Abdolmaleki  
42 et al. 2021). It might, however, take several decades for a fully autonomous transportation system  
43 to be deployed. Many experts argue that even with a fully developed and comprehensively tested  
44 AV technology, there will still be individuals who either have a distrust in the technology or do not  
45 wish to cease driving for other personal reasons. Therefore, it is safe to assume that AVs would  
46 have to share the roadway network with human drivers for the unforeseeable future.

47 Since the advent of personal automobiles traffic engineers have been interested in studying the  
48 car-following behaviour of human drivers, with Bruce Greenshields being credited with the first  
49 recorded set of experiments to scientifically measure this car-following behaviour (Greenshields

50 et al. 1934). The advent of AVs has given rise to an interesting research question: Will the car-  
51 following behaviour of human drivers be affected when they knowingly follow an autonomous  
52 vehicle? Few attempts have been made in the literature to answer this question. (Rahmati et al.  
53 2019) set up two sets of experiments with a platoon of size three, where the third vehicle in the  
54 platoon was a human-driven vehicle. In the first set of experiments, the second vehicle was a human-  
55 driven vehicle, and in the second set of experiments it was an AV. They recorded the trajectory of  
56 the third vehicle, and used data-driven and model-based approaches to discern any changes in the  
57 car-following behaviour of the third vehicle in reaction to its preceeding vehicle. They concluded  
58 that when following an AV, a human driver's car-following behaviour is significantly different than  
59 following a human-driven vehicle.

60 Conducting controlled field experiments allows for assessing the impact of a single factor at  
61 a time on the car-following behaviour of human drivers, while keeping all other factors fixed.  
62 However, controlled field experiments have a number of downsides. First, a combinatorial number  
63 of experiments are required to capture the impact of multiple factors changing at once. This  
64 could easily render comprehensive controlled field experiments impractical, since a wide range of  
65 environmental factors as well as the presence of other agents (e.g., other AVs or legacy vehicles,  
66 pedestrians, bicycles, etc.) may play a role in the car-following behaviour of drivers. As a result,  
67 the conclusions obtained from basic and contained field experiments, although insightful, may not  
68 be readily generalizable to a naturalistic driving environment. As such, in this paper we seek to  
69 investigate the car-following behavior of human drivers who follow an AV in a naturalistic driving  
70 environment using a naturalistic and large dataset that allows for making statistically significant  
71 conclusions. To this end, we use the Lyft Level 5 (Lyft L5) (Houston et al. 2020) data repository, in  
72 which a fleet of AVs travels on a fixed route in an urban environment, providing over 1,000 hours of  
73 AV trajectories, their surrounding agents, and the transportation network. The route encompasses  
74 a variety of transportation facility types, including intersections and corridors. This dataset is the  
75 first to enable analysis of the car-following behaviour of a heterogeneous set of drivers who follow  
76 an AV in a naturalistic and dynamically changing driving environment.

77 Despite the benefits of using naturalistic driving data in analyzing the changes in the car-  
78 following behaviour of human drivers when following an AV, it also poses a unique set of challenges.  
79 More specifically, the appearance of an AV is a key factor that can influence a human driver's car-  
80 following behavior. For the presence of an AV to change the behaviour of human drivers, they  
81 should be able to discern that they are following an AV based on clear visual cues. Garnished by  
82 lidars and cameras, AVs generally have a distinctive look that human drivers are likely to discern.  
83 Additionally, a human driver's car-following behaviour depends on their subjective opinion on how  
84 an AV operates and its risk-taking attitude (Zhao et al. 2020). As such, to mitigate the risk of  
85 unwanted bias in data collection, data should be collected within an extended period of time from  
86 a diverse set of drivers.

87 The car-following behaviour of a driver can be reflected using a number of parameters, e.g.,  
88 velocity, acceleration, and time headway (Wang et al. 2014). Here, we use time headway (THW)—  
89 defined as the time it takes for the following vehicle to reach its leading vehicle—to model car-  
90 following behaviour. As such, we conduct change point analysis on THW of the following driver  
91 to identify the moment in time when the human driver has identified its leading AV.

92 The remainder of the paper is organized as follows. We first present the existing work and  
93 list the contributions of this paper in the LITERATURE REVIEW section. Then, we provide the  
94 analytical approach in detail. After that, we lay out our analysis using Lyft L5 and NGSIM datasets  
95 and present our findings in the RESULTS AND DISCUSSION section. Finally, we conclude the  
96 paper by summarizing our findings.

## 97 **LITERATURE REVIEW**

98 In traffic modeling, car-following behavior has been intensively studied to establish how a  
99 vehicle interacts with its leading vehicle. The main idea is to work with longitudinal dynamics  
100 of the vehicle pair, such as velocity, acceleration, time headway, and time-to-collision inverse, to  
101 uncover the behavior patterns of the following vehicle in various driving scenarios. There are two  
102 main components involved in the study of car-following behavior: modeling and analysis. These  
103 two components are discussed in the following.

104 **Modeling**

105 As the most commonly encountered driving maneuver in the real world, car-following behavior  
106 has been extensively studied in investigating many specific driving scenarios. To properly describe  
107 the interaction between the leading and following vehicles, several measures are proposed. Time-  
108 to-collision (TTC) reflects human drivers' perception of their safety for potential collision, and it is  
109 strongly related to longitudinal acceleration/deceleration (Jin et al. 2011). (Vogel 2003) compares  
110 time headway and TTC with real-world traffic data and concludes that time headway and TTC are  
111 independent but suitable for different usages. They also argue that time headway directly reflects  
112 potential danger and thus prevents risky TTC, while TTC should be used for actual danger, i.e.,  
113 on-road obstacle or collision. (Boer 1999) also mentioned that time headway characterizes the  
114 safety margin in the situation where the preceding vehicle decelerates, while TTC denotes the time  
115 left for drivers to intervene to avoid a crash. Headway is not considered here as it can not include  
116 velocity-related information, which is necessary to learn the car-following behavior. As we are  
117 interested in human drivers' reaction to on-road stimuli (the preceding AV) without evaluating an  
118 actual collision, in our study we select time headway to model the car-following behaviour.

119 Several car-following behavior models are formulated using ordinary differential equations  
120 (ODE) that take positions and velocities of vehicles as inputs. The intelligent driving model (IDM)  
121 (Treiber et al. 2000) and optimal velocity model (OVM) (Sugiyama 1999) are two extensively-  
122 applied ODE-based models capable of modeling nonlinear dynamics. Additionally, a linearized  
123 model can be further derived from ODEs via Taylor expansion. The full velocity difference model  
124 (FVDM) (Jiang et al. 2001) was developed based on OVM and the generalized force model (GFM)  
125 (Helbing and Tilch 1998) by taking both positive and negative velocity differences into account.  
126 It could obtain more precise predictions of vehicle motion in traffic jam density. Wiedemann  
127 74 (W-74) model and Wiedemann 99 (W-99) model (Durrani et al. 2016) are two car-following  
128 models developed by Rainer Wiedemann, where the drivers change their behaviors at discrete time  
129 steps only when certain thresholds (predefined for headway, speed, or relative speed) are reached.  
130 However, the values of parameters in W-99 are empirical, and no literature exists to indicate how

ranges for these parameter should be established, which prompted many related works (Durrani et al. 2016; Mathew and Radhakrishnan 2010; Gallelli et al. 2017) in calibrating the W-99 model. Newell's car-following model (Newell 2002) applied a similar concept to W-99, assuming that a vehicle will maintain a minimum space and time gap between itself and its preceding vehicle. Some studies which pursue a more general way of modeling the car-following behavior are discussed in (Ro et al. 2017; Koutsopoulos and Farah 2012), where not only the car-following dynamics is considered, but also random human factors and different driving scenarios (such as following and emergency braking) were accounted for. Other car-following models such as adaptive cruise control (ACC) and cooperative adaptive cruise control (CACC) were designed for commercial vehicles, applying automated longitudinal control by adjusting acceleration with a linear function to maintain preset velocity and headway values.

All of the aforementioned car-following models are based on mathematical formulations with longitudinal dynamics, taking advantage of traditional control theory. On the other hand, predictive techniques enable a data-driven approach and can directly learn the car-following behavior using real-world data. (Zhang et al. 2008) utilized time headway and time-to-collision inverse data and a back-propagation neural network to reproduce longitudinal accelerations. A long short-term memory (LSTM) neural network in (Zhang et al. 2019) used the position information of surrounding vehicles to predict the car-following behavior with low longitudinal trajectory error. A deep deterministic policy gradient reinforcement learning car-following model was developed in (Zhu et al. 2018), where a mapping from speed, relative speed, and headway to acceleration regime of the following vehicle were obtained to deliver a human-like car-following model. A Gaussian mixture model (GMM) was developed in (Angkititrakul et al. 2011) to anticipate the future car-following behavior based on velocity and headway. Such learning-based methods require a large amount of training data, and the quality of data significantly influences model performance. Neural network-based designs also require careful tuning when learning the longitudinal dynamics of vehicles (Da Lio et al. 2020).

From the literature, it can be noticed that multiple longitudinal dynamics impact the car-

158 following behaviors of both the following vehicle and the proceeding vehicle, among which relative  
159 distance and velocity are the two most essential factors. To leverage this finding and reduce the  
160 complexity of the model, we select time headway as the main feature for modeling car-following  
161 behavior as it accounts for both relative distance and velocity (Chen et al. 2015; Vogel 2002).

## 162 Analysis

163 Car-following behavior is of interest to transportation researchers as it can provide insights into  
164 the best ways to approach flow throughput control, on-road safety, and energy consumption, etc.  
165 There are two directions followed in the current literature to analyze the car-following behavior of  
166 drivers: one studies the stability (string stability and plant stability) of traffic flow, while the other  
167 quantifies the car-following behavior using statistical tools such as mean and variance. As this work  
168 focuses on patterns of interactions between human-driven vehicles and AVs, the analysis of string  
169 stability and plant stability is out of the scope this study.

170 Car-following behavior may be affected by many factors such as road condition, weather, and  
171 vehicle type. When dealing with data relevant to multiple factors, Analysis of Variance (ANOVA)  
172 is a powerful tool to investigate the influence level of each factor. In (Liu et al. 2019), two one-way  
173 ANOVA tests were conducted, indicating that different speed limits have a significant influence on  
174 the time headway and headway, and the mean of time headway is closely centered around a fixed  
175 value. A factorial ANOVA analysis was conducted in (Hjelkrem 2015) to determine the interactions  
176 between area type, number of lanes, and vehicle type influencing the car-following behavior. Road  
177 condition is suggested to be a critical factor in influencing both headway and time headway by  
178 (Wang et al. 2015; Houchin 2015). Significant influence from vehicle type (2-door car v.s. 4-door  
179 vehicles, sedans v.s. trucks, vehicles v.s. motorcycles) is also observed in (Evans and Wasielewski  
180 1983; Houchin 2015; Amini et al. 2019).

181 The literature on the analysis of car-following behavior mainly focuses on human-driven ve-  
182 hicles, and AV-involved scenarios are rarely studied. Human-AV interactions at the microscopic  
183 level were first studied in (Rahmati et al. 2019), where a field experiment was conducted though  
184 setting up two two-vehicle platoon structures of human-following-human and human-following-

185 AV. (Rahmati et al. 2019) showed that a shorter headway is selected when human drivers follow  
186 an AV. Other field experiments conducted by (Zhao et al. 2020) suggest that a driver's subjective  
187 attitude toward to AV technology dominates the actual AV's driving behavior in the speed-headway  
188 relationship. Observations from these two field experiments indicate that the limited data collected  
189 from field experiments degrades the robustness of the intersection effect(s). Recently, (Li et al.  
190 2021) leveraged the Lyft L5 dataset as the data source for operational safety analysis in human-AV  
191 interactions in car-following scenarios. In this study we utilize the Lyft L5 and NGSIM datasets  
192 to provide a comprehensive and robust evaluation of the car-following behaviour of humans, ac-  
193 counting for multiple factors that may affect the car-following behaviour of human drivers. This  
194 naturalistic study serves as a necessary complement to the existing field experiments.

## 195 Contribution

196 The objective of this paper is to provide insights on the potential influence of AVs on the  
197 car-following behavior of human drivers. The contributions of this paper are two-fold: *(i)* we  
198 conduct statistical analysis on time headway data from Lyft L5, using NGSIM datasets (US101, I-  
199 80, Lankershim Blvd) as the control group, to find the influence of leading AVs on the car-following  
200 behaviour of following drivers; *(ii)* This naturalistic study provides evidence that human drivers  
201 are regulated as a result of introducing AVs, as evidenced by the statistically significant reduction  
202 in the mean value and variance of their time headways.

## 203 METHODS

204 The objective of this study is to investigate whether, and the extent to which, the existence of  
205 AVs in the traffic stream influences the car-following behaviour of human drivers. To answer this  
206 question, we propose a comprehensive framework demonstrated in Figure 1. Data used in this study  
207 is obtained from two public datasets: Lyft L5 (Houston et al. 2020) and NGSIM (NGS 2021). We  
208 use time headway time series in our analysis as a proxy to quantify the car-following behaviour of  
209 vehicles. Time headway between two vehicles is defined as the travel time from the centroid of the  
210 following vehicle to the centroid of the preceding/leading vehicle based on the following vehicle's  
211 speed. In the rest of this paper, we denote a legacy vehicle following an autonomous vehicle as

212 LFA, and a legacy vehicle following a legacy vehicle as LFL. We refer to LFA and LFL as platoon  
213 structures.

214 As displayed in Figure 1, the proposed framework consists of two main phases, namely, data  
215 acquisition and data analysis. These phases are described in the following sections.

## 216 **Phase I: Data Acquisition**

217 The first phase starts by extracting time headways of LFL and LFA platoon structures. More  
218 precisely, we extract LFA time headways from the Lyft L5 dataset, and LFL time headways from  
219 both Lyft L5 and NGSIM datasets. Once the time headways are extracted, We use Bayesian change  
220 point analysis to filter out the portions of time headway data in the LFA platoon structure where  
221 the legacy vehicle is not aware of following an AV.

### 222 *Change Point Analysis*

223 Our objective in this study is to make a determination on whether the presence of an AV affects  
224 the car-following behaviour of its following vehicle in the LFA platoon structure. Consequently,  
225 we first need to identify scenarios in the Lyft L5 dataset where a legacy vehicle is following an  
226 AV, and more importantly, is *aware* that it is following an AV. To identify such scenarios, we first  
227 identify scenes from the Lyft L5 dataset where a legacy vehicle is immediately following an AV.  
228 Next, for each scene we conduct change point analysis to mark any changes in the time headway  
229 sequence of the legacy vehicle and the velocity sequence of its leading AV. The adopted Change  
230 point analysis is an online detection approach that provides uncertainty bounds on the number and  
231 location of change points across observations (Ruggieri and Antonellis 2016). This method strives  
232 to make fast inferences on the occurrence of new change points based on each new observation.

233 Let us denote by  $c_L^h$  the time instance when a change point is detected in the time headway  
234 time series of the legacy vehicle, and by  $c_A^v$  the time instance when a change point identified in  
235 the velocity time series of the AV. Let us denote by  $t_{\min}^r$  and  $t_{\max}^r$  the minimum and maximum  
236 reaction time of the legacy vehicle, i.e., the time period lapsed from the moment the AV changes  
237 its acceleration and the moment the acceleration of the legacy vehicle changes in response. When  
238  $t_{\min}^r \leq c_L^h - c_A^v \leq t_{\max}^r$ , the change in the time headway of the legacy vehicle can be attributed

239 to its car-following behaviour. However, when  $c_L^h$  is not proceeded with a  $c_A^v$  within the time  
240 interval  $[t_{\min}^r, t_{\max}^r]$ , i.e., the change point analysis detects a change in time headway of the legacy  
241 vehicle that cannot be attributed to its car-following behaviour, we postulate that this change can be  
242 attributed to the legacy vehicle having identified its proceeding vehicle as an AV, and only consider  
243 the trajectory of the legacy vehicle after this change point. In other instances where no such change  
244 point is detected, we assume that the legacy vehicle is aware of its leading AV due to the distinctive  
245 appearance of AVs in the Lyft L5 study.

246 Owing to many factors, such as the driving environment, age, gender, and experience, the  
247 range for the reaction time can vary from case to case, as shown in (Johansson and Rumar 1971;  
248 McGehee et al. 2000; Summala 2000), where different field experiments and calibrated models  
249 find the minimum value ( $t_{\min}^r$ ) can be as small as 0.3 seconds, and the maximum value ( $t_{\max}^r$ ) can  
250 be as high as 2.4 seconds. Avoiding the extreme values where reaction times may slightly increase  
251 when the stimulus (e.g., following an AV instead of another legacy vehicle) is a surprise to drivers  
252 (Johansson and Rumar 1971; Mehmoor and Easa 2009), or decrease at lower driving speeds (Calvi  
253 et al. 2018; Ruhai et al. 2010), in this study we set the minimum and maximum values of reaction  
254 time to  $t_{\min}^r = 0.5$  and  $t_{\max}^r = 1$  seconds, respectively, following the literature.

255 For human drivers, there is a preferable time headway interval towards the preceding vehicle  
256 (Fuller 1981; Das and Maurya 2017). The preferable time headway is the most frequently adopted  
257 time headway when human drivers are in the car-following mode, which is used to baseline the  
258 car-following behavior of rational human drivers. Following the existing literature (e.g., (WINSUM  
259 and Heino 1996; Van Winsum and Brouwer 1997; Van Winsum 1998; Bham' and Ancha 2006)),  
260 the preferable time headway is considered to be 1 to 2.5 seconds in this study. When time headway is  
261 shorter than the lower bound, drivers are more likely to slow down, while when the time headway is  
262 longer than the upper bound, drivers may either keep the current speed or accelerate to catch up with  
263 the preceding vehicle. The basic idea is that when the time headway is inside the interval, human  
264 drivers will feel comfortable and will not overreact unless there is an external disturbance. This  
265 preferable time headway may be influenced by many factors (e.g., road configuration, lane, etc.).

266 Generally, there is no universal standard, and this interval can be determined from the observed  
267 data itself. We use the distribution of time headway in the LFA dataset to define the preferable time  
268 headway.

269 In the final step of phase I, the collected and filtered time headways from both Lyft L5 and  
270 NGSIM datasets are integrated and associated. In this step, each time headway is labeled based on  
271 platoon structure, road type, time period, data source, and lane, as shown in Figure 2.

272 **Phase II: Analysis**

273 Phase II focuses on analysis. In the first step, two samples of equal sizes are taken from LFA  
274 and LFL datasets. Next, partial autocorrelation analysis is employed to detect autocorrelation lags.  
275 Using these identified lags, differencing is applied to stationarize the randomly selected time series.  
276 Next, we define the factors of interest, which alongside time headway will be used for fitting the  
277 ANOVA model.

278 Once the factors of interest are identified and before fitting the nested model, we first create  
279 balanced datasets.

280 To obtain balanced datasets we sample time headways without replacement from LFL and LFA  
281 datasets so that the same number of data points will be available in each branch of the nested design.  
282 Next, the ANOVA model is fitted using balanced datasets. Finally, we confirm the adequacy of the  
283 fitted model, and conduct follow-up pair-wise comparisons to isolate the effects that are significantly  
284 different, as displayed in Figure 1. The major steps of the analysis are detailed in the following.

285 **Analysis of Variance**

286 Analysis of Variance (ANOVA) is one of the most well-known statistical tools for evaluating the  
287 existence of significant differences between factor levels on a continuous measurement (Tabachnick  
288 and Fidell 2013). A factorial ANOVA can be implemented to examine the impacts of independent  
289 categorical factors on a continuous target variable. Factorial ANOVA is an suitable approach to  
290 study whether there exists a statistically significant difference in the time headway patterns of LFA  
291 and LFL platoon structures based on different factors and their levels. One of the main requirements  
292 of ANOVA is the independence of observations. The underlying sequential and time dependant

293 nature of time series data is a direct violation of this requirement. To address this issue, we apply  
294 a two-step data processing procedure. First, we randomly (without replacement) down-sample the  
295 time series to remove any potential dependencies. Next, we render the randomly selected time  
296 series approximately stationary through differencing to remove auto-correlation.

297 *Stationarity and Partial Auto-Correlation*

298 In time series, auto-correlation is the correlation between two observations at different time  
299 stamps, where these observations correlate with themselves repetitively at certain lags. Auto-  
300 correlation and partial auto-correlation plots can be used to study the auto-correlation of time series.  
301 Although auto-correlation plots can measure and visualize the correlation between observations  
302 for a predefined set of lags, they fail to account for the propagation of correlation among successive  
303 lags. Partial auto-correlation analysis addresses this problem by isolating the auto-correlation  
304 lag. In this work, we use partial auto-correlation plots to identify auto-correlation lags, and apply  
305 differencing at the identified lags to stationarize the time headway time series. We discard data  
306 points that cannot be stationarized by first level differencing.

307 *Nested Fixed Effect Model*

308 The design of the fitted factorial ANOVA is highly dependent on the structure of the collected data.  
309 Fig. 2 displays the factors of interest. A total of five factors are considered in this study. The first  
310 factor, platoon structure, models whether the reported time headway profiles belong to an LFL or  
311 an LFA pair. The second factor, road type, represents whether the data is collected from an urban  
312 road network (i.e., Palo Alto, CA and Lankershim Blvd, CA) or a freeway (i.e., US 101, CA and  
313 I-80, CA). The third factor, time period, models whether the data is collected during the morning  
314 (i.e., 7:50am - 9:00am) or afternoon (i.e., 4:00pm - 5:30pm) peak period.

315 The fourth factor studies whether the source of the collected data has any significant impact on  
316 human driving behavior. Data source is defined as a factor to account for the impact of different  
317 data collection techniques and locations in NGSIM and Lyft L5 datasets. The final factor, lane,  
318 represents the lane at which the data has been collected. This factor is considered because the  
319 lane in which a vehicle travels could impact its car-following behaviour. As the number of lanes is

320 different across data collection sites, we used one-way ANOVA to group lanes that failed to show a  
 321 statistically significant difference in their car-following behaviour based on time headway analysis.  
 322 As a result, the lane levels simplified to the left (i.e., speeding) lane, the middle lanes, and the right  
 323 (merging) lane. Note that the high occupancy vehicle lanes were filtered out in this study when  
 324 present.

325 The factorial ANOVA relies on the underlying relationships between these different factors.  
 326 Note that AVs are only present in the Lyft L5 dataset and the Lyft L5 data is limited to an urban  
 327 environment. Furthermore, AV trajectories only appear on the right lane. As such, the values of the  
 328 factors data source, lane, and road type are restricted to the values of the factor platoon structure,  
 329 leading to the choice of a nested factorial ANOVA as shown in Equation (1).

$$Y_{l(ijknm)} = \mu + \alpha_i + \beta_j + (\alpha \times \beta)_{ij} + \gamma_{k(j)} + \lambda_{m(j)} + \theta_{n(j)} + \epsilon_{l(ijknm)},$$

for  $i, j, k, m \in \{1, 2\}$  and  $n \in \{1, 2, 3\}$  (1)

330 where  $\mu$  represents the overall mean, and  $\alpha_i, \beta_j, \gamma_{k(j)}, \lambda_{m(j)}$ , and  $\theta_{n(j)}$  capture the effects of  
 331 time period, platoon structure, data source, road type, and lane, respectively. The parenthetical  
 332 subscriptions illustrate the nesting structure of the model. The  $(\alpha \times \beta)_{ij}$  models the interaction  
 333 effects between factors time period and platoon structure. Here,  $\epsilon_{l(ijknm)}$  represents the error term,  
 334 which is assumed to follow  $N(0, \sigma^2)$ . In addition to the normality and constant assumptions

335 regarding the error term, the fitted model should also satisfy the following constraints:

$$\sum_i \alpha_i = 0 \quad (2a)$$

$$\sum_j \beta_j = 0 \quad (2b)$$

$$\sum_i (\alpha \times \beta)_{ij} = 0, \quad \forall j \in \{1, 2\} \quad (2c)$$

$$\sum_j (\alpha \times \beta)_{ij} = 0, \quad \forall i \in \{1, 2\} \quad (2d)$$

$$\sum_k \gamma_{k(j)} = 0, \quad \forall j \in \{1, 2\} \quad (2e)$$

$$\sum_m \lambda_{m(j)} = 0, \quad \forall j \in \{1, 2\} \quad (2f)$$

$$\sum_n \theta_{n(j)} = 0, \quad \forall j \in \{1, 2\} \quad (2g)$$

336 As the nested factorial model in Equation (1) is not identifiable, the additional sets of constraints  
337 in Equation (2) help narrow down the solution space to a unique set of fitted parameters. Using a  
338 single ANOVA model, we define several hypotheses tests to assess the significance of each factor,  
339 with the null hypothesis in each case indicating that the mean time headways are similar for different  
340 values of a given factor, and the alternative hypothesis indicating otherwise.

341 Nested factors (i.e., data source, lane, and road type) are added to absorb some of the unexplained  
342 variability. As a result, specific hypothesis tests associated with nested factors are of lesser  
343 importance.

344 Although a rejection of the null hypothesis in the ANOVA analysis signals the existence of  
345 a significant effect (i.e., factor), it fails to identify the factor level that is significantly different,  
346 specifically in the presence of interaction effects. As a result, ANOVA analyses are usually followed  
347 by pairwise comparisons. While studying the effects of multiple factor levels, comparisons between  
348 the individual means of either factor may be made using any pairwise comparison technique. We  
349 use Least Square Means to investigate the significance of the factors and apply Tukey's HSD method  
350 to adjust the significance level (Abdi and Williams 2010).

351        Multiple assumptions are made prior to fitting the nested fixed effect model. As a result, the  
352        adequacy of the model relies on whether these assumptions hold true. These assumptions include  
353        1) the normality of the residuals, i.e.,  $\epsilon_{l(ijknm)} \sim N(0, \sigma^2)$ , and 2) the homogeneity of the residuals.  
354        Many mathematical tests are developed for checking the normality and homogeneity of the residuals  
355        (e.g., the Shapiro-Wilk test ). One problem with such tests is that as the sample size increases, the  
356        test results are more likely to fail for even minor departures from normality or homoscedasticity.  
357        Therefore, in this paper we rely on visualization approaches instead.

## 358        **DATA**

359        The raw data within both repositories are collected using different sensors such as digital video  
360        cameras, radars and lidars.

### 361        **Lyft L5 Dataset**

362        The Lyft L5 Prediction data repository was released by the Lyft Level 5 team in June 2020  
363        (Houston et al. 2020). This data repository contains raw camera/lidar/radar data collected from a  
364        fleet of 23 AVs operating along a fixed high-demand route in Palo Alto, CA, from October 2019 to  
365        March 2020. An internal perception stack has already been applied to report information such as  
366        the vehicle position based on a global coordinate system, velocity, and a unique ID for each agent.  
367        We extract the time headway series of each legacy vehicle for the purpose of this study.

### 368        **NGSIM Dataset**

369        The Next Generation Simulation (NGSIM) is a well-known dataset published by the U.S.  
370        Department of Transportation Intelligent Transportation Systems Joint Program Office (JPO) (NGS  
371        2021). This dataset includes detailed vehicle trajectory data collected in four sites: southbound  
372        US 101 and Lankershim Boulevard in Los Angeles, CA, eastbound I-80 in Emeryville, CA, and  
373        Peachtree Street in Atlanta, Georgia. The data is collected in different time periods from April 20,  
374        2005 to November 9, 2006. The dataset contains vehicle ID, global coordinates of the vehicle,  
375        vehicle type, velocity, acceleration, space headway, and time headway, among other attributes. We  
376        extract the time headway series of each vehicle in each regular (non-carpool) lane at each site for

377 the purpose of this study.

378 **Data Processing Pipeline**

379 To fully leverage the abundant data in the Lyft L5 and NGSIM datasets for ANOVA, a modular  
380 data processing pipeline is developed with three blocks: time headway calculation, change point  
381 analysis, and down-sampling and filtering. A detailed explanation of the processing pipeline is  
382 given for the Lyft L5 dataset.

- 383 • Time headway calculation: Realizing that the driving behavior in different lanes on the  
384 same road may be different, the lane-specific time headway data is of interest to us. To  
385 stay consistent with the NGSIM dataset, all the raw data in the Lyft L5 dataset is taken  
386 from the multi-lane roads. By utilizing the provided semantic map with 8,500 discrete lane  
387 segments, a customized semantic map is constructed by connecting any lanes that physically  
388 belong to the same continuous lane (multiple lane segments in the original semantic map  
389 may correspond to the same lane in the real world), referred as the augmented map. In  
390 the multi-lane roads, three lane groups are identified (right, middle, and left). Given the  
391 position information of vehicles, the augmented map can immediately match vehicles to the  
392 corresponding lane groups. The time headway in the car-following mode is calculated as the  
393 travel time from the centroid of the following vehicle to the centroid of the preceding/leading  
394 vehicle based on the following vehicle's speed.
- 395 • Change point analysis: In investigating an AV's effect on the following behaviour of human  
396 drivers, we need to construct a dataset in which the following human driver is aware that  
397 the leading vehicle is an AV. To this end, we conduct a change point analysis as described  
398 in section CHANGE POINT ANALYSIS.
- 399 • Down-sampling and filtering: The sampling frequency in both datasets is 10 Hz, and a high  
400 correlation among data points is present under such a high-frequency sampling regime.  
401 To ensure independence of observations, autocorrelation and partial autocorrelation are  
402 evaluated, and down-sampling of the time headway sequence is implemented. According to

403 our evaluation results, 1 Hz is selected to be the updated sampling frequency. Furthermore,  
404 a filtering step is introduced to ensure that the time headway sequence satisfies the minimum  
405 length of containing at least 10 data points or 10-seconds of observation.

406 For the NGSIM dataset, as the lane information is readily available, only the down-sampling  
407 and filtering module will be used.

## 408 RESULTS AND DISCUSSION

409 In this section, we present the results of our proposed framework. In accordance with the flow  
410 of the framework, we first stationarize the time headway time series through differencing and partial  
411 auto-correlation analysis. Then, we balance our dataset. Next, we test our hypotheses using nested  
412 factorial ANOVA, followed by pairwise comparisons.

### 413 Down-sampling and Auto-correlation Analysis

414 Since the sample frequency in Lyft L5 and NGSIM datasets is high (10 Hz), data points may  
415 correlate with each other at such high frequency and thus introduce unnecessary bias into the  
416 results. A common approach to reduce autocorrelation is to down-sample the data at a slower  
417 frequency. We test Autocorrelation Function (ACF) and Partial Autocorrelation Function (PACF)  
418 at down-sampling frequencies of 2Hz and 1Hz, in comparison with the original data. Decreasing  
419 sample frequency can significantly reduce both ACF and PACF at higher lags. Down-sampling  
420 at 1 Hz can reduce the magnitude of the auto-correlation lags. Differencing at lag one further  
421 stationarizes the time series. As the majority of the time series are not significantly auto-correlated  
422 after lag 1 differencing, the non-stationary ones are dropped at this step.

423 Some interesting takeaways may be discussed before presenting the ANOVA results. In a  
424 freeway driving environment, e.g., US 101 and I-80, after down-sampling at 1 Hz, there is still  
425 a significant autocorrelation at lag 1 and neutrally-distributed partial autocorrelation (PAC) after  
426 lag 2. In an urban driving environment, Lankershim Blvd and Lyft L5, a similar pattern can  
427 be observed; however, at lag 1, a relative smaller ratio of data is correlated. An interpretation  
428 for this difference is that in freeways, human drivers encounter fewer external disturbances and

429 therefore their behavior is more consistent and predictable. A neutral-distributed outbound PAC  
430 after lag 2 indicates that the behaviors tend to be random in 2 seconds into the future. If we view  
431 a human driver as a controller, s/he will control the time headway to the leading vehicle roughly at  
432 some period, which can be determined by the lag where outbound PAC values are approximately  
433 neutral-distributed.

#### 434 **Factorial Analysis**

435 The processed dataset contains a total of 537,060 data points, out of which 5,774 (i.e., 1%)  
436 of data points represent the LFA structure while the remaining 531,285 (i.e., 99%) belong to the  
437 LFL platoon structure. In order to maximize the power of the factorial analysis, the dataset should  
438 be balanced. In addition, balancing helps protect the analysis against small departures from the  
439 assumptions. Although the balancing effort reduces the total size of the dataset (i.e., 25 data points  
440 per each leaf in Figure 2) through random sampling, it improves the the distribution of the data  
441 within different factor levels, including platoon structure: 85% for LFL and 15% LFA; Road type:  
442 46% for freeway and 54% urban; Time period: 53% for morning and 45% afternoon; Lane: 31%  
443 for left, 31% for middle and 38% right.

444 The nested factorial ANOVA introduced in Equation 1 is fitted and its results are displayed in  
445 Table 1. The fitted model allows us to study whether there are statistically significant associations  
446 between the time headway and the factors introduced in Figure 1. Table 1 reports findings on the  
447 main effects (i.e., time period and platoon structure factors), nested effects (i.e., data source, road  
448 type, and lane factors), as well the interaction effects between the time period and platoon structure  
449 factors.

450 The first three rows in Table 1 correspond to hypotheses on time period, platoon structure,  
451 and the interaction effect between time period and platoon structure factors. The next three rows  
452 display the impact of data source, road type, and lane as nested factors of platoon structure,  
453 respectively. The last row provides information regarding the residuals. For each one of the  
454 hypotheses of interest, Table 1 reports the degree of freedom (DoF) of the test, sum of squared  
455 errors (SSE), mean square errors (MSE), as well as the F-statistics, its corresponding p-value,

456 and the significance level at which a conclusion is made. The reported p-values can assess the  
457 null hypotheses and determine whether the association between the time headway and the factors  
458 of interest are statistically significant. Table 1 reports that only the platooning structure is of  
459 significance at  $\alpha = 0.001$ . The results also highlights the fact that the collected time headway  
460 data are not impacted by the differences in data collection techniques and locations in NGSIM and  
461 Lyft L5 datasets at a statistically significant level. To further study the results reported in Table 1,  
462 multiple follow up pairwise comparisons are conducted to understand which levels of the platoon  
463 structure factor are significantly different given the nested structure. Table 2 illustrates the results  
464 of the pairwise comparisons.

465 Although the platoon structure is the only significant factor as reported in Table 1, the interaction  
466 effect between time period and platoon structure and the nesting factors may have obscured the  
467 comparisons between the means of different levels of the platoon structure. As a result, the least  
468 squared method is applied to the means of one of the factors, with the remaining factor set at a  
469 particular level. In addition, as pairwise comparisons lead to inflation of the significance level, the  
470 p-values within Table 2 are adjusted based on the Tukey method for comparing a family of multiple  
471 estimators.

472 Table 2 reports the estimated difference between means (i.e., estimate), the standard error of  
473 that estimate (i.e., SE), the T ratio, and its corresponding p-value along with the reported level of  
474 significance  $\alpha$ . The top half of Table 2 studies the pairwise comparisons between time period and  
475 platoon structure. Here, results are averaged over the levels of lane (i.e., left, middle, and right),  
476 road type (i.e., freeway and urban), and data source (i.e., NGSIM and Lyft L5). As shown in Table  
477 2, when the same platoon structure is present (e.g., Morning LFL - Afternoon LFL and Morning  
478 LFA - Afternoon LFA), no significant difference is observed in the mean time headway. Otherwise,  
479 the remaining pairwise comparisons between time period and platoon structure are significant.

480 The bottom half of Table 2 studies the interaction between the nested factor lane and the main  
481 factor platoon structure. Here, results are averaged over the levels of time period (i.e., morning  
482 and afternoon), road type (i.e., freeway and urban), and data source (i.e., NGSIM and Lyft L5).

483 This table demonstrates that: (1) LFL behavior does not significantly differ within the middle, left,  
484 and right lane groups; (2) LFL behavior significantly differs within the left, middle, and right lane  
485 groups when compared to LFA in the right lane; (3) LFL and LFA display statistically different  
486 behaviors in different lanes; and (4) LFL and LFA display statistically different behaviors within  
487 the right lane.

488 Although the proposed nested factorial model recognizes that the factor platoon structure leads to  
489 a statistically significant different car-following behaviour, and the follow-up pair-wise comparisons  
490 further confirm this, none of these approaches can identify whether the THW of LFA is less than  
491 or greater than LFL's THW. Figure 3 demonstrates that LFL has higher mean and variance THW  
492 values when compared to LFA.

493 As displayed in Figure 3, LFA has lower median (1.38), mean (0.41), and variance (0.31) THW  
494 values in comparison to the median (2.48), mean (0.85), and variance (1.05) of THW in LFL.  
495 The reduction in the mean time headway manifests in less bumper-to-head distance, enabling more  
496 vehicles to operate on the road and increasing road capacity. The reduction in the variance of time  
497 headway leads to a more stable traffic flow.

498 The final step is the verification of the fitted model's adequacy through Q-Q and residuals plots  
499 as shown in Figure 4. To check the adequacy of the model, Q-Q plots of residuals and residuals  
500 versus fitted values are shown in Figure 4. Q-Q plots are commonly used to confirm the normality  
501 of the residuals, i.e.,  $\epsilon_{l(ijknm)} \sim N(0, \sigma^2)$ . As a Q-Q plot is a scatter plot created by plotting the  
502 actual quantiles of the residuals of the fitted model against the theoretical normally distributed ones,  
503 a diagonal line is a confirmation that both sets of quantiles came from the same distribution. In the  
504 Q-Q plot in Figure 4, the residuals roughly lie around the 45-degree line, suggesting that they are  
505 approximately normally distributed. The homogeneity of the residuals can be validated using the  
506 residuals plot. If the variance of the error term is homogeneous, not only should the residuals plot  
507 show no pattern, but also the spread of residuals should be equal per group across corresponding  
508 fitted values. The residuals plot in Figure 4 shows that the variances are approximately homogeneous  
509 since the residuals are distributed approximately equally above and below zero.

510 **CONCLUSIONS**

511 In this study we proposed a nested factorial model to study the potential effects of AVs on human  
512 drivers' car-following behavior using naturalistic driving data (i.e., NGSIM and Lyft L5 prediction  
513 datasets). The objective of this study was to bridge the gap between anticipated and real-world  
514 impacts of AVs on traffic streams and roadway capacity. The proposed nested model studied the  
515 impact of different factors such as platoon structure (i.e., whether a human driver follows a legacy  
516 vehicle or an AV), time period, traveling lane, and road type on the time headway between two  
517 vehicles, which is considered as a proxy for the car-following behaviour of the following vehicle.  
518 The results indicate that the platoon structure affects the car-following behavior of human drivers  
519 in a statistically significant manner, allowing us to conclude that in a real-world setting, a human  
520 driver's car-following behaviour when following a legacy vehicle is different from following an AV.  
521 Furthermore, our analysis illustrates that the difference in the car-following behaviour of human  
522 drivers is significantly present regardless of the traveling lane or the time period.

523 **DATA AVAILABILITY STATEMENT**

524 Some of models, or code that support the findings of this study are available from the corre-  
525 sponding author upon reasonable request; All data used during the study are available in repositories  
526 online in accordance with the funder's data retention policies.

527 **ACKNOWLEDGMENTS**

528 This work has been supported by Midwest US-DOT Center for Connected and Automated  
529 Transportation (award number: 69A3551747105) and National Science Foundation (award number:  
530 1837245).

531 **REFERENCES**

532 (2021). "U.s. department of transportation federal highway administration. (2016) next generation  
533 simulation (ngsim) vehicle trajectories and supporting data. [dataset]. provided by its datahub  
534 through data.transportation.gov.

535 Abdi, H. and Williams, L. J. (2010). "Tukey's honestly significant difference (hsd) test." *Encyclo-*  
536 *pedia of research design*, 3(1), 1–5.

537 Abdolmaleki, M., Shahabi, M., Yin, Y., and Masoud, N. (2021). "Itinerary planning for cooperative  
538 truck platooning." *Transportation Research Part B: Methodological*, 153, 91–110.

539 Amini, E., Tabibi, M., Khansari, E. R., and Abhari, M. (2019). "A vehicle type-based approach  
540 to model car following behaviors in simulation programs (case study: Car-motorcycle following  
541 behavior)." *IATSS research*, 43(1), 14–20.

542 Angkititrakul, P., Miyajima, C., and Takeda, K. (2011). "Modeling and adaptation of stochas-  
543 tic driver-behavior model with application to car following." *2011 IEEE Intelligent Vehicles*  
544 *Symposium (IV)*, IEEE, 814–819.

545 Bham', G. H. and Ancha, S. R. P. (2006). "Statistical models for preferred time headway and  
546 time headway of drivers in steady state car-following." *Applications of Advanced Technology in*  
547 *Transportation*, 344–349.

548 Boer, E. R. (1999). "Car following from the driver's perspective." *Transportation Research Part F:*  
549 *Traffic Psychology and Behaviour*, 2(4), 201–206.

550 Calvi, A., Benedetto, A., and D'Amico, F. (2018). "Investigating driver reaction time and speed dur-  
551 ing mobile phone conversations with a lead vehicle in front: A driving simulator comprehensive  
552 study." *Journal of Transportation Safety & Security*, 10(1-2), 5–24.

553 Chen, X. M., Li, L., and Shi, Q. (2015). "A markov model based on headway/spacing distributions."  
554 *Stochastic Evolutions of Dynamic Traffic Flow*, Springer, 49–79.

555 Da Lio, M., Bortoluzzi, D., and Rosati Papini, G. P. (2020). "Modelling longitudinal vehicle  
556 dynamics with neural networks." *Vehicle System Dynamics*, 58(11), 1675–1693.

557 Das, S. and Maurya, A. K. (2017). "Time headway analysis for four-lane and two-lane roads."  
558 *Transportation in developing economies*, 3(1), 9.

559 Durrani, U., Lee, C., and Maoh, H. (2016). "Calibrating the wiedemann's vehicle-following model  
560 using mixed vehicle-pair interactions." *Transportation research part C: emerging technologies*,  
561 67, 227–242.

562 Ersal, T., Kolmanovsky, I., Masoud, N., Ozay, N., Scruggs, J., Vasudevan, R., and Orosz, G. (2020).  
563     “Connected and automated road vehicles: state of the art and future challenges.” *Vehicle system*  
564     *dynamics*, 58(5), 672–704.

565 Evans, L. and Wasielewski, P. (1983). “Risky driving related to driver and vehicle characteristics.”  
566     *Accident Analysis & Prevention*, 15(2), 121–136.

567 Fuller, R. G. (1981). “Determinants of time headway adopted by truck drivers.” *Ergonomics*, 24(6),  
568     463–474.

569 Gallelli, V., Iuele, T., Vaiana, R., and Vitale, A. (2017). “Investigating the transferability of  
570     calibrated microsimulation parameters for operational performance analysis in roundabouts.”  
571     *Journal of Advanced Transportation*, 2017.

572 Greenshields, B. D., Thompson, J., Dickinson, H., and Swinton, R. (1934). “The photographic  
573     method of studying traffic behavior.” *Highway Research Board Proceedings*, Vol. 13.

574 Helbing, D. and Tilch, B. (1998). “Generalized force model of traffic dynamics.” *Physical review*  
575     *E*, 58(1), 133.

576 Hjelkrem, O. A. (2015). “Determining influential factors on the threshold of car-following behav-  
577     ior.” *Report no.*

578 Houchin, A. J. (2015). “An investigation of freeway standstill distance, headway, and time gap data  
579     in heterogeneous traffic in iowa.

580 Houston, J., Zuidhof, G., Bergamini, L., Ye, Y., Chen, L., Jain, A., Omari, S., Iglovikov, V., and  
581     Ondruska, P. (2020). “One thousand and one hours: Self-driving motion prediction dataset.”  
582     *arXiv preprint arXiv:2006.14480*.

583 Jiang, R., Wu, Q., and Zhu, Z. (2001). “Full velocity difference model for a car-following theory.”  
584     *Physical Review E*, 64(1), 017101.

585 Jin, S., Huang, Z.-y., Tao, P.-f., and Wang, D.-h. (2011). “Car-following theory of steady-state traffic  
586     flow using time-to-collision.” *Journal of Zhejiang University-SCIENCE A*, 12(8), 645–654.

587 Johansson, G. and Rumar, K. (1971). “Drivers’ brake reaction times.” *Human factors*, 13(1), 23–27.

588 Koutsopoulos, H. N. and Farah, H. (2012). “Latent class model for car following behavior.”

589        *Transportation research part B: methodological*, 46(5), 563–578.

590        Li, T., Han, X., Ma, J., Ramos, M., and Lee, C. (2021). “Operational safety of automated and  
591        human driving in mixed traffic environments: A perspective of car-following behavior.” *Pro-*  
592        *ceedings of the Institution of Mechanical Engineers, Part O: Journal of Risk and Reliability*,  
593        1748006X211050696.

594        Liu, T. et al. (2019). “Comparison of car-following behavior in terms of safety indicators between  
595        china and sweden.” *IEEE Transactions on Intelligent Transportation Systems*, 21(9), 3696–3705.

596        Liu, X., Masoud, N., and Zhu, Q. (2020a). “Impact of sharing driving attitude information: A  
597        quantitative study on lane changing.” *2020 IEEE Intelligent Vehicles Symposium (IV)*, IEEE,  
598        1998–2005.

599        Liu, X., Zhao, G., Masoud, N., and Zhu, Q. (2020b). “Trajectory planning for connected and  
600        automated vehicles: Cruising, lane changing, and platooning.” *arXiv preprint arXiv:2001.08620*.

601        Masoud, N. and Jayakrishnan, R. (2017). “Autonomous or driver-less vehicles: Implementation  
602        strategies and operational concerns.” *Transportation research part E: logistics and transportation*  
603        *review*, 108, 179–194.

604        Mathew, T. V. and Radhakrishnan, P. (2010). “Calibration of microsimulation models for nonlane-  
605        based heterogeneous traffic at signalized intersections.” *Journal of Urban Planning and Devel-*  
606        *opment*, 136(1), 59–66.

607        McGehee, D. V., Mazzae, E. N., and Baldwin, G. S. (2000). “Driver reaction time in crash  
608        avoidance research: Validation of a driving simulator study on a test track.” *Proceedings of the*  
609        *human factors and ergonomics society annual meeting*, Vol. 44, Sage Publications Sage CA: Los  
610        Angeles, CA, 3–320.

611        Mehmood, A. and Easa, S. M. (2009). “Modeling reaction time in car-following behaviour based on  
612        human factors.” *International Journal of Civil and Environmental Engineering*, 3(9), 325–333.

613        Newell, G. F. (2002). “A simplified car-following theory: a lower order model.” *Transportation*  
614        *Research Part B: Methodological*, 36(3), 195–205.

615        Rahmati, Y., Khajeh Hosseini, M., Talebpour, A., Swain, B., and Nelson, C. (2019). “Influence

616 of autonomous vehicles on car-following behavior of human drivers.” *Transportation research*  
617 *record*, 2673(12), 367–379.

618 Ro, J. W., Roop, P. S., Malik, A., and Ranjitkar, P. (2017). “A formal approach for modeling and  
619 simulation of human car-following behavior.” *IEEE transactions on intelligent transportation*  
620 *systems*, 19(2), 639–648.

621 Ruggieri, E. and Antonellis, M. (2016). “An exact approach to bayesian sequential change point  
622 detection.” *Computational Statistics & Data Analysis*, 97, 71–86.

623 Ruhai, G., Weiwei, Z., and Zhong, W. (2010). “Research on the driver reaction time of safety  
624 distance model on highway based on fuzzy mathematics.” *2010 International Conference on*  
625 *Optoelectronics and Image Processing*, Vol. 2, IEEE, 293–296.

626 Stern, R. E., Cui, S., Delle Monache, M. L., Bhadani, R., Bunting, M., Churchill, M., Hamilton,  
627 N., Pohlmann, H., Wu, F., Piccoli, B., et al. (2018). “Dissipation of stop-and-go waves via  
628 control of autonomous vehicles: Field experiments.” *Transportation Research Part C: Emerging*  
629 *Technologies*, 89, 205–221.

630 Sugiyama, Y. (1999). “Optimal velocity model for traffic flow.” *Computer Physics Communications*,  
631 121, 399–401.

632 Summala, H. (2000). “Brake reaction times and driver behavior analysis.” *Transportation Human*  
633 *Factors*, 2(3), 217–226.

634 Tabachnick, B. G. and Fidell, L. S. (2013). “Using multivariate statistics upper saddle river.

635 Treiber, M., Hennecke, A., and Helbing, D. (2000). “Congested traffic states in empirical observa-  
636 tions and microscopic simulations.” *Physical review E*, 62(2), 1805.

637 Van Winsum, W. (1998). “Preferred time headway in car-following and individual differences in  
638 perceptual-motor skills.” *Perceptual and motor skills*, 87(3), 863–873.

639 Van Winsum, W. and Brouwer, W. (1997). “Time headway in car following and operational  
640 performance during unexpected braking.” *Perceptual and motor skills*, 84(3\_suppl), 1247–1257.

641 Vogel, K. (2002). “What characterizes a “free vehicle” in an urban area?.” *Transportation research*  
642 *part F: traffic psychology and behaviour*, 5(1), 15–29.

643 Vogel, K. (2003). "A comparison of headway and time to collision as safety indicators." *Accident*  
644 *analysis & prevention*, 35(3), 427–433.

645 Wang, J., Xiong, C., Lu, M., and Li, K. (2015). "Longitudinal driving behaviour on different  
646 roadway categories: an instrumented-vehicle experiment, data collection and case study in  
647 china." *IET Intelligent Transport Systems*, 9(5), 555–563.

648 Wang, W., Xi, J., and Chen, H. (2014). "Modeling and recognizing driver behavior based on driving  
649 data: A survey." *Mathematical Problems in Engineering*, 2014.

650 WINSUM, W. V. and Heino, A. (1996). "Choice of time-headway in car-following and the role of  
651 time-to-collision information in braking." *Ergonomics*, 39(4), 579–592.

652 Wyk, F. v., Khojandi, A., and Masoud, N. (2019). "A path towards understanding factors affecting  
653 crash severity in autonomous vehicles using current naturalistic driving data." *Proceedings of  
654 SAI Intelligent Systems Conference*, Springer, Cham, 106–120.

655 Zhang, E., Masoud, N., Bandegi, M., Lull, J., and Malhan, R. K. (2022a). "Step attention: Sequen-  
656 tial pedestrian trajectory prediction." *IEEE Sensors Journal*, 22(8), 8071–8083.

657 Zhang, E., Masoud, N., Bandegi, M., and Malhan, R. K. (2022b). "Predicting risky driving in a  
658 connected vehicle environment." *IEEE Transactions on Intelligent Transportation Systems*.

659 Zhang, E., Pizzi, S., and Masoud, N. (2021). "A learning-based method for predicting heterogeneous  
660 traffic agent trajectories: implications for transfer learning." *2021 IEEE International Intelligent  
661 Transportation Systems Conference (ITSC)*, IEEE, 1853–1858.

662 Zhang, L., Wang, J., Li, K., Yamamura, T., Kuge, N., and Nakagawa, T. (2008). "Driver car-  
663 following behavior modeling using neural network based on real traffic experimental data." *15th  
664 World Congress on Intelligent Transport Systems and ITS America's 2008 Annual MeetingITS  
665 AmericaERTICOITS JapanTransCore*.

666 Zhang, X., Sun, J., Qi, X., and Sun, J. (2019). "Simultaneous modeling of car-following and lane-  
667 changing behaviors using deep learning." *Transportation research part C: emerging technologies*,  
668 104, 287–304.

669 Zhang, Z., Tafreshian, A., and Masoud, N. (2020). "Modular transit: Using autonomy and modular-

670        ity to improve performance in public transportation.” *Transportation Research Part E: Logistics*  
671        and *Transportation Review*, 141, 102033.

672        Zhao, X., Wang, Z., Xu, Z., Wang, Y., Li, X., and Qu, X. (2020). “Field experiments on longitudinal  
673        characteristics of human driver behavior following an autonomous vehicle.” *Transportation*  
674        *research part C: emerging technologies*, 114, 205–224.

675        Zhu, M., Wang, X., and Wang, Y. (2018). “Human-like autonomous car-following model with deep  
676        reinforcement learning.” *Transportation research part C: emerging technologies*, 97, 348–368.

677	<b>List of Tables</b>	
678	1	Results of the nested fixed model . . . . . 29
679	2	Pairwise comparisons using least square means . . . . . 30

**TABLE 1.** Results of the nested fixed model

Factor	DoF	SSE	MSE	F Statistics	P-Value	$\alpha$
Time Period	1	1.46	1.46	1.55	0.21	
Platoon Structure	1	49.86	49.86	52.81	2.88e-12	0.001
Platoon Structure $\times$ Time	1	1.09	1.09	1.16	0.28	
Platoon Structure: Data Source	1	0.03	0.03	0.04	0.85	
Platoon Structure: Road Type	1	1.92	1.92	2.03	0.15	
Platoon Structure: Lane	2	0.01	0.006	0.006	0.99	
Residuals	317	299.28	0.94			

**TABLE 2.** Pairwise comparisons using least square means

	Estimate	SE	T Ratio	P-Value	$\alpha$
Time Period (Morning vs Afternoon) : Platoon Structure (LFL vs LFA)					
Morning LFL - Afternoon LFL	-0.132	0.132	-0.996	0.7519	
Morning LFL - Morning LFA	0.944	0.215	4.39	0.0001	0.001
Morning LFL - Afternoon LFA	1.055	0.215	4.91	<.0001	0.001
Afternoon LFL - Morning LFA	1.075	0.218	4.93	<.0001	0.001
Afternoon LFL - Afternoon LFA	1.187	0.218	5.44	<.0001	0.001
Morning LFA - Afternoon LFA	0.112	0.275	0.40	0.9774	
Lane (Left vs Middle vs Right) : Platoon Structure (LFL vs LFA)					
Left LFL - Middle LFL	0.013	0.138	0.098	0.9997	
Left LFL - Right LFL	0.016	0.158	-0.103	0.9996	
Left LFL - Right LFA	1.073	0.0171	6.279	<.0001	0.001
Middle LFL - Right LFL	-0.003	0.160	-0.022	1.000	
Middle LFL - Right LFA	1.061	0.171	6.279	<.0001	0.001
Right LFL - Right LFA	1.057	0.191	6.20	<.0001	0.001

680 **List of Figures**

681	1	The proposed framework to study the car-following behavior of drivers in LFL and	
682		LFA platoon structures. . . . .	32
683	2	The Structure of the proposed nested model. . . . .	33
684	3	The distribution of time headway over factor levels. . . . .	34
685	4	Adequacy check of the fitted nested fixed effect model: (a) Q-Q plot; and (b)	
686		residuals v.s. fitted values . . . . .	35

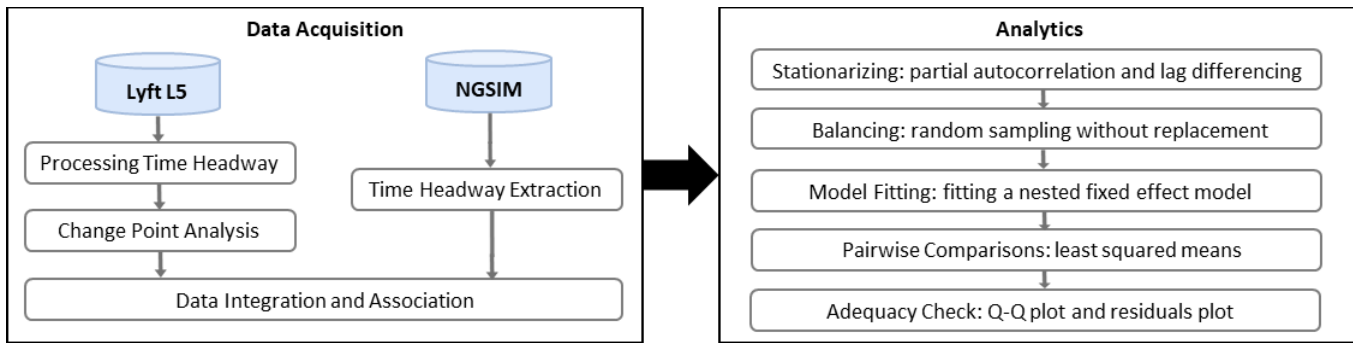


**Fig. 1.** The proposed framework to study the car-following behavior of drivers in LFL and LFA platoon structures.

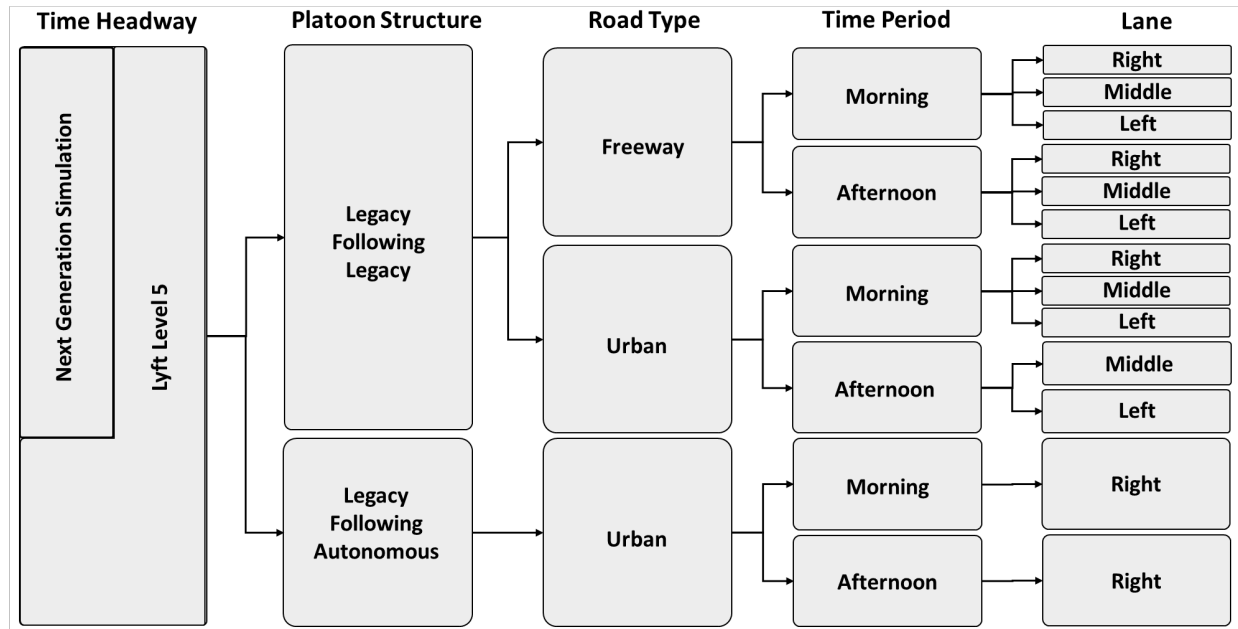


**Fig. 2.** The Structure of the proposed nested model.

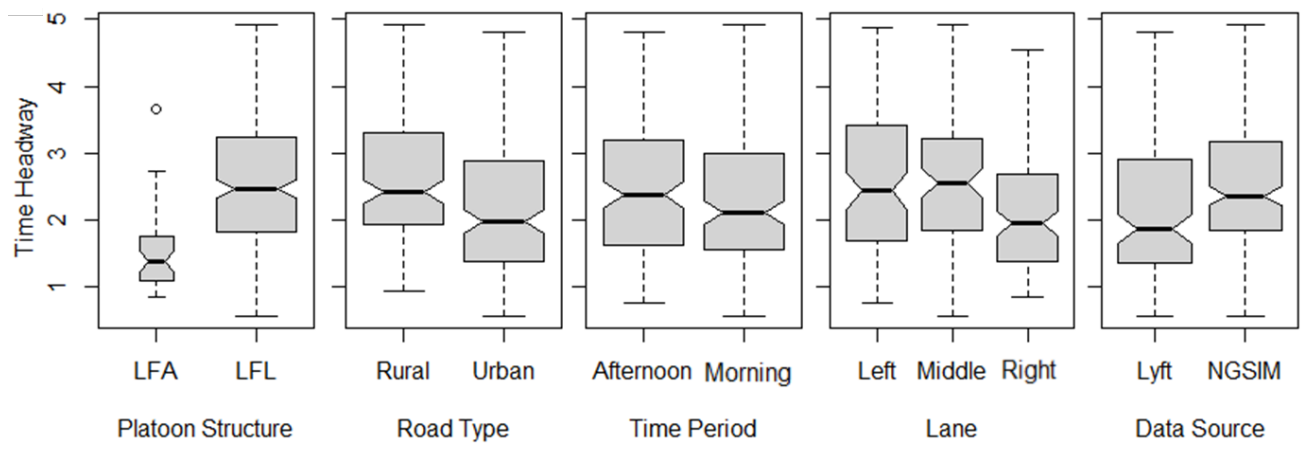
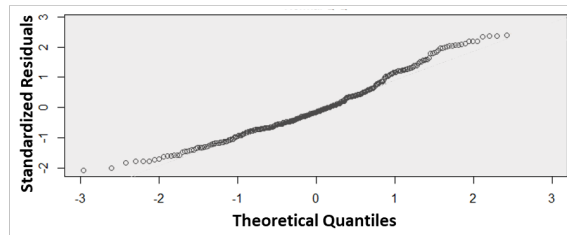
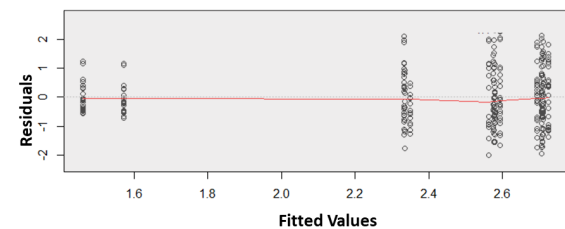


**Fig. 3.** The distribution of time headway over factor levels.



(a)



(b)

**Fig. 4.** Adequacy check of the fitted nested fixed effect model: (a) Q-Q plot; and (b) residuals v.s. fitted values